reference mass spectrum of unlabeled propane and that of the labeled mixture. It is assumed that the "isotope effect"[86] does not influence the fragmentation process. A part of the reference spectrum $m_1$ to $m_7$ have relative intensities $I_1$ to $I_7$ as shown in Figure 9.

From the measured peaks $p_1$ to $p_4$ of the labeled mixture, one can calculate the fractions $f_1$ to $f_4$. Each of the measured intensities $p$ is the sum of the fraction multiplied by the intensity of the unlabeled component. This follows from Figure 9 and is shown in eq 1:

$$p_1 = I_1 f_1 + I_2 f_2 + I_3 f_3 + I_4 f_4 \quad (1)$$

This can be written in matrix form for all the four peaks measured:

$$\begin{pmatrix} P_1 \\ p_2 \\ p_3 \\ P_4 \end{pmatrix} = \begin{pmatrix} I_1 & I_2 & I_3 & I_4 \\ I_2 & I_3 & I_4 & I_5 \\ I_3 & I_4 & I_5 & I_6 \\ I_4 & I_5 & I_6 & I_7 \end{pmatrix} \begin{pmatrix} f_1 \\ f_2 \\ f_3 \\ f_4 \end{pmatrix} \quad (2)$$

The fractions $f_1$ to $f_4$ are calculated from the inverse matrix ($\mathbf{M}^{-1}$) containing the intensities $I_1$ to $I_7$ from eq 2:

$$\vec{f} = \mathbf{M}^{-1} \cdot \vec{p} \quad (3)$$

Finally the fractions $f_i$ ($i$ = 1-4) are normalized according to:

$$f_i = f_i / \sum_{i=1}^{4} f_i \quad (4)$$

In principle, from any $n$ peaks from the mass spectrum of $C_nH_{2n+2}$ this calculation can be performed; however, experimental errors are relatively low when differences between intensities in the reference spectrum are large. Therefore, we used the masses $m/z$ 44-47 for propane, $m/z$ 30-32 for ethane, and $m/z$ 31-29 for the $C_2$ fragment of propane. By comparing the analyses of the $C_2$ and the $C_3$ fragments of propane, it could be concluded that in the singly labeled product mainly the primary atom is labeled.

**Acknowledgment.** We gratefully thank Henri M. J. Snijders for his assistance at the high resolution mass spectrometer and Jef L. Willigers for his experimental help at the microflow reactor. The Dutch Organisation of Fundamental Chemical Research, SON, is acknowledged for its financial support.

**Registry No.** $CH_4$, 74-82-8; $C_2H_4$, 74-84-0; $C_2H_2$, 74-86-2; $C_3H_8$, 115-07-1; $CH_3CH_2CH_3$, 74-98-6; $CH_3(CH_2)_2CH_3$, 106-97-8; $CH_3(CH_2)_3CH_3$, 109-66-0; $^{13}CH_4$, 6532-48-5; $CH_3{}^{13}CH_3$, 6145-17-1; $^{13}CH_3{}^{13}CH_3$, 52026-74-1; $CH_3CH_2{}^{13}CH_3$, 17251-65-9; $CH_3{}^{13}CH_2CH_3$, 17251-62-6; $CH_3(CH_2)_2{}^{13}CH_3$, 22612-53-9; $CH_3CH_2{}^{13}CH_2{}^{13}CH_3$, 141556-21-0; $CH_3(^{13}CH_2)_2{}^{13}CH_3$, 141556-22-1; ruthenium, 7440-18-8; cobalt, 7440-48-4.

# Aerobic Oxidative Dehydrogenations Catalyzed by the Mixed-Addenda Heteropolyanion $PV_2Mo_{10}O_{40}^{5-}$: A Kinetic and Mechanistic Study

**Ronny Neumann* and Michal Levin**

*Contribution from the Casali Institute of Applied Chemistry, Graduate School of Applied Science and Technology, The Hebrew University of Jerusalem, Jerusalem, Israel 91904.*
*Received December 31, 1991*

**Abstract:** The aerobic oxidative dehydrogenation of $\alpha$-terpinene to $p$-cymene catalyzed by the mixed-addenda heteropolyanion $PV_2Mo_{10}O_{40}^{5-}$ has been used to investigate the oxidation mechanism catalyzed by this class of compounds. The kinetics of the reaction show it to be zero order in $\alpha$-terpinene, first order in dioxygen, and second order in the heteropolyanion catalyst. The kinetic results along with the use of UV-vis, ESR, $^{31}P$ NMR, and IR spectroscopy have enabled the formulation of a reaction scheme involving the formation of a stable substrate-catalyst complex in the catalyst reduction (substrate oxidation) stage and a $\mu$-peroxo catalyst intermediate in the catalyst reoxidation stage where dioxygen is reduced to water in a four-electron redox reaction.

## Introduction

Since the discovery in 1826 by Berzelius of the first heteropoly compound,[1] the vast field of heteropolyanion chemistry has been centered mostly around the preparation, structure, properties, and analytical chemistry applications of these compounds.[2] Heteropoly compounds are soluble polyoxoion salts of anions having the general formula $[X_xM_mO_y]^{q-}$ ($x \leq m$), where X is a heteroatom and M is an addenda atom. A common and important class of these salts and those used in the majority of catalytic applications is the Keggin compounds (Figure 1), with the general formula $XM_{12}O_{40}^{q-}$ (**1**) (X = P, Si, As, Ge, B, etc.; M = Mo, W). Further catalytically important subclasses of the Keggin compounds are the mixed-addenda anions $XM'_nM_{12-n}O_{40}^{q-}$ (**2**), where for example X = P, M' = V, and $n$ = 1, 2, and the transition metal substituted Keggin compounds $XM'(L)M_{11}O_{39}$ (**3**), where M' is a transition metal such as Mn, Co, Cu, Ru, etc. and L is a ligand such as $H_2O$, OH, or pyridine, among others.

Interest in heteropoly compounds as homogeneous liquid-phase oxidation catalysts is only a recent development that has been fueled by the inherent stability of these compounds to strongly oxidizing conditions as opposed to other effective and widely studied catalysts such as metalloporphyrins,[3] which always decompose in the presence of oxidants.[4] Importantly, it has also

(1) Berzelius, J. *Pogg. Ann.* **1826**, *6*, 369, 380.
(2) (a) Pope, M. T. *Heteropoly and Isopoly Oxometallates*; Springer: Berlin, 1983. (b) Tsigdinos, G. A. *Top. Curr. Chem.* **1978**, *76*, 1. (c) Day, V. W.; Klemperer, W. G. *Science* **1985**, *228*, 533. (d) Pope, M. T.; Müller, A. *Angew. Chem., Int. Ed. Engl.* **1991**, *30*, 34.
(3) Ortiz de Montellano, P. R. *Cytochrome P-450*; Plenum: New York, 1986.
(4) Recently efforts have been made to increase the stability of porphyrins by halogenation of the porphyrin ring: (a) Traylor, T. G.; Tsuchiya, S. *Inorg. Chem.* **1987**, *26*, 1339. (b) Traylor, T. G.; Byun, Y. S.; Traylor, P. S.; Bationi, P.; Mansuy, D. *J. Am. Chem. Soc.* **1991**, *113*, 7821.

0002-7863/92/1514-7278$03.00/0 

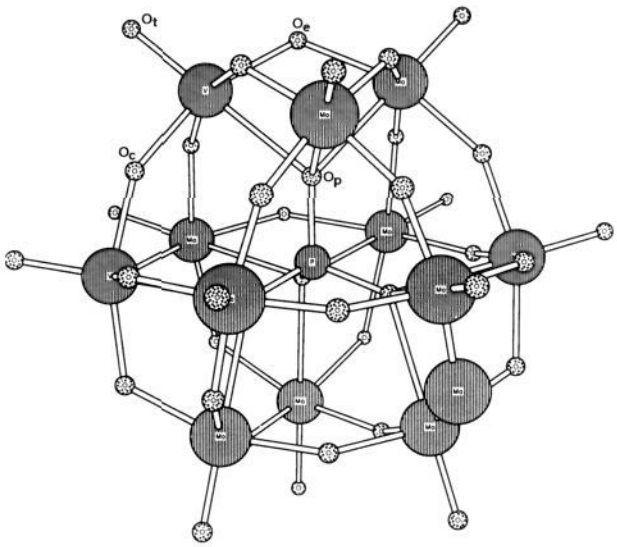


**Figure 1.** Ball and stick drawing of the $PV_2Mo_{10}O_{40}$ heteropolyanion showing the 1,6 isomer and the different types of oxygen atoms.

been found that these catalysts are effective in utilizing ecologically favored oxidants such as dioxygen and hydrogen peroxide. Four general but somewhat different approaches have been taken in the use of heteropolyanions in catalytic liquid-phase oxidations. The first approach has been to use polyoxotungstates, **1** (X = P; M = W), with dioxygen in photochemically catalyzed oxidative dehydrogenations of alkanes to alkenes[5] and alcohols to ketones.[6] These reactions are initiated by ultraviolet light excitation of the polyoxotungstate. The second type of liquid-phase oxidation catalysis has been performed with molybdenum or tungsten Keggin heteropolyanions, **1** (X = Si, P; M = Mo, W), with nonsymmetric quaternary ammonium countercations (e.g. hexadecylpyridinium) as catalysts in oxidations of alcohols,[7] allyl alcohols,[8] alkenes,[9] alkynes,[10] $\beta$-unsaturated acids,[11] *vic*-diols,[12] and phenol[13] with hydrogen peroxide. These reactions are very typical of molybdenum and tungsten centers in general, and recent evidence indicates that at least in some of these systems the true catalysts are not heteropolyoxometalates but instead simpler $PO_4[WO(O_2)_2]_4^{3-}$ peroxo compounds formed in situ.[14] A third category of reactions is one where the transition metal substituted heteropolyoxometalates, **3**, are used as catalysts. Conceptually in these compounds a transition metal, M′, is complexed by an inorganic ligand, such as the lacunary or deficient heteropolyoxometalate $XM_{11}O_{39}^{9-}$. Reactions take place at the transition metal center; these catalysts are sometimes viewed as inorganic analogues of metalloporphyrins.[15] This approach has been realized for cobalt and manganese in the epoxidation of alkenes with iodosobenzene,[16] the hydroxylation of alkanes with *tert*-butyl hydroperoxide,[17] and the autoxidation of hindered phenols with dioxygen.[18] For ruthenium as the catalytic transition metal center, the oxidation of alkenes and alkanes has been performed with a variety of oxidants, yielding a range of product selectivities.[19]

A fourth approach and the one discussed in this paper has been to use mixed-addenda heteropolyoxomolybdates, **2**, usually $PV_2Mo_{10}O_{40}^{5-}$, as catalysts in liquid-phase oxidation electron transfer or redox type oxidations according to the simplified reaction scheme shown in eq 1. In general, these oxidations are

$$\text{substrate} + \text{Cat}_{ox} \rightarrow \text{product} + \text{Cat}_{red} + 2H^+$$

$$\text{Cat}_{red} + 2H^+ + \tfrac{1}{2}O_2 \rightarrow \text{Cat}_{ox} + H_2O \qquad (1)$$

visualized to proceed by transfer of electrons and protons from the substrate to the catalyst in the first stage, yielding product and a protonated and reduced catalyst. In the second stage, the reduced catalyst is reoxidized in the presence of dioxygen, yielding water and completing the catalytic cycle. Substrates in these reactions are *not oxygenated*, and in the context of the above reaction scheme, they may be organic molecules as in the dehydrogenation and aromatization of dienes,[20] the oxidative dehydrogenation of alcohols and amines,[21] and the oxidative coupling of dialkylphenols to diphenoquinones.[22] Substrates may also be inorganic species such as those used in the oxidation of bromide amions to molecular bromine[23] or primary catalysts such as Pd(0) (product is Pd(II)) in Wacker-type oxidations of ethylene to acetaldehyde[24] or the acetoxylation of aromatics.[25] Certain cases have also been documented where the $H_5PV_2Mo_{10}O_{40}$ heteropolyacid has been used in *oxygenation* reactions such as the oxidation of sulfides to sulfoxides and sulfones[26] and the oxidative cleavage of ketones[27] and diols.[28] It is probable, however, that these latter reactions are best interpreted as being catalyzed by oxovanadium(IV) acid complexes.[29]

Although a significant body of synthetic applications using the mixed-addenda heteropolyoxovanadomolybdates has now been

(5) (a) Fox, M. A.; Cardona, R.; Gaillard, E. *J. Am. Chem. Soc.* **1987**, *109*, 6347. (b) Nomiya, K.; Sugie, Y.; Miyazaki, T.; Miwa, M. *Polyhedron* **1986**, *5*, 1267. (c) Hill, C. L.; Bouchard, D. A. *J. Am. Chem. Soc.* **1985**, *107*, 5148.

(6) (a) Renneke, R. F.; Hill, C. L. *J. Am. Chem. Soc.* **1988**, *110*, 5461. (b) Renneke, R. F.; Hill, C. L. *New J. Chem.* **1987**, *11*, 763. (c) Renneke, R. F.; Hill, C. L. *J. Am. Chem. Soc.* **1986**, *108*, 3528. (d) Renneke, R. F.; Hill, C. L. *Angew. Chem., Int. Ed. Engl.* **1988**, *27*, 1526. (e) Chambers, R. C.; Hill, C. L. *Inorg. Chem.* **1989**, *28*, 2511.

(7) (a) Yamawaki, K.; Yoshida, T.; Nishihara, H.; Ishii, Y.; Ogawa, M. *Synth. Commun.* **1986**, *16*, 53. (b) Daumas, M.; Vo-Quang, Y.; Vo-Quang, L.; *Le Goffic, F. Synthesis* **1989**, *64*.

(8) Matoba, Y.; Inoue, H.; Akagi, J.; Okabayashi, T.; Ishii, Y.; Ogawa, M. *Synth. Commun.* **1984**, *14*, 865.

(9) (a) Ishii, Y.; Yamawaki, K.; Ura, T.; Yamada, H.; Yoshida, T.; Ogawa, M. *J. Org. Chem.* **1988**, *53*, 3587. (b) Furukawa, H.; Nakamura, T.; Inagaki, H.; Nishikawa, E.; Imai, C.; Misono, M. *Chem. Lett.* **1988**, 877. (c) Schwegler, M.; Floor, M.; van Bekkum, H. *Tetrahedron Lett.* **1988**, *29*, 823. (d) Venturello, C.; D'Aloiso, R.; Bart, J. C. J.; Ricci, M. *J. Mol. Catal.* **1985**, *32*, 107.

(10) Balistreri, F. P.; Failla, S.; Spina, E.; Tomaselli, G. A. *J. Org. Chem.* **1989**, *54*, 947.

(11) Oguchi, T.; Sakata, Y.; Takeuchi, N.; Kaneda, K.; Ishii, Y.; Ogawa, M. *Chem. Lett.* **1989**, 2053.

(12) Sakata, Y.; Ishii, Y. *J. Org. Chem.* **1991**, *56*, 6233.

(13) (a) Shimuzu, M.; Takehira, K.; Hayakawa, T.; Orita, H. *Jpn. Kokai Tokkyo Koho* JP 01,238,552. (b) Shimizu, M.; Orita, H.; Hayakawa, T.; Watanabe, Y.; Takehira, K. *Bull. Chem. Soc. Jpn.* **1991**, *64*, 2583.

(14) (a) Brégeault, J.-M.; Aubry, C.; Chottard, G.; Platzer, N.; Chauveau, F.; Huet, C.; Ledon, H. In *Dioxygen Activation and Homogeneous Catalytic Oxidation*; Simandi, L. I., Ed.; Elsevier: Amsterdam, 1991; p 521. (b) Aubry, C.; Chottard, G.; Platzer, N.; Brégeault, J.-M.; Thouvenot, R.; Chauveau, F.; Huet, C.; Ledon, H. *Inorg. Chem.* **1991**, *30*, 4409.

(15) (a) Katsoulis, D. E.; Pope, M. T. *J. Am. Chem. Soc.* **1984**, *106*, 2737. (b) Hill, C. L. *Activation and Functionalization of Alkanes*; Wiley: New York, 1989. (c) Mansuy, D.; Bartoli, J.-F.; Battioni, P.; Lyon, D. K.; Finke, R. G. *J. Am. Chem. Soc.* **1991**, *113*, 7222.

(16) Hill, C. L.; Brown, R. B. *J. Am. Chem. Soc.* **1986**, *108*, 536.

(17) Faraj, M.; Hill, C. L. *J. Chem. Soc., Chem. Commun.* **1987**, 1487.

(18) Katsoulis, D. E.; Pope, M. T. *J. Chem. Soc., Dalton Trans.* **1989**, 1483.

(19) (a) Neumann, R.; Abu-Gnim, C. *J. Chem. Soc., Chem. Commun.* **1989**, *1324*. (b) Neumann, R.; Abu-Gnim, C. *J. Am. Chem. Soc.* **1990**, *112*, 6025.

(20) Neumann, R.; Lissel, M. *J. Org. Chem.* **1989**, *54*, 4607.

(21) Neumann, R.; Levin, M. *J. Org. Chem.* **1991**, *56*, 5707.

(22) Lissel, M.; Jansen in de Wal, H.; Neumann, R. *Tetrahedron Lett.* **1992**, *33*, 1795.

(23) Neumann, R.; Assael, I. *J. Chem. Soc., Chem. Commun.* **1988**, 1285.

(24) (a) Kozhevnikov, I. V.; Matveev, K. I. *Russ. Chem. Rev.* (*Engl. Transl.*) **1978**, *47*, 1231. (b) Matveev, K. I.; Kozhevnikov, I. V. *Kinet. Catal.* (*Engl. Transl.*) **1980**, *21*, 855.

(25) Rachovskaya, L. N.; Matveev, K. I.; Il'inich, G. N.; Ermenko, N. K. *Kinet. Catal.* (*Engl. Transl.*) **1977**, *18*, 854.

(26) Kozhevnikov, I. V.; Simagna, V. I.; Varnakova, G. V.; Matveev, K. I. *Kinet. Katal.* **1979**, *20*, 506.

(27) (a) El Ali, B.; Brégeault, J.-M.; Mercier, J.; Martin, J.; Martin, C.; Convert, O. *J. Chem. Soc., Chem. Commun.* **1989**, 825. (b) El Ali, B.; Brégeault, J.-M.; Martin, J.; Martin, C. *New J. Chem.* **1989**, *13*, 825.

(28) Brégeault, J.-M.; El Ali, B.; Mercier, J.; Martin, J.; Martin, C. *C. R. Acad. Sci., Ser. 2* **1989**, *309*, 459.

(29) Brégeault, J.-M.; El Ali, B.; Mercier, J.; Martin, J.; Martin, C.; Mohammedi, O. In *New Developments in Selective Oxidation*; Centi, G., Trifirò, F., Eds.; Elsevier: Amsterdam, 1990; p 205.

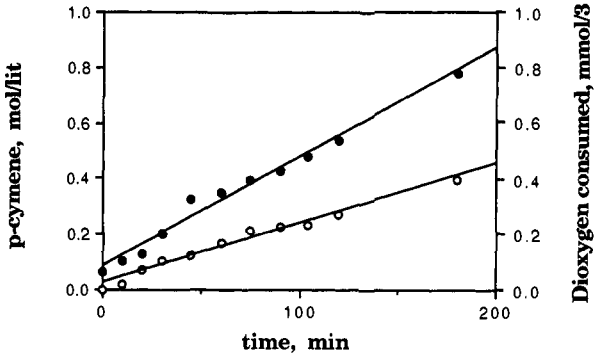


**Figure 2.** Reaction profile of α-terpinene oxidative dehydrogenation showing both *p*-cymene formation and dioxygen consumption. Reaction conditions: 3 mmol of α-terpinene and 0.0375 mmol of $H_5PV_2Mo_{10}O_{40}$ in 3 mL of acetonitrile at a dioxygen pressure of 0.94 atm at 25 °C.

developed, only little is known about the mechanistic aspects of these catalytic oxidative dehydrogenations. In this paper we describe our mechanistic investigations into a simple but typical model oxidative dehydrogenation reaction: the aerobic oxidative dehydrogenation of α-terpinene to *p*-cymene catalyzed by the $PV_2Mo_{10}O_{40}^{5-}$ heteropolyanion, eq 2. Thus, both kinetic and

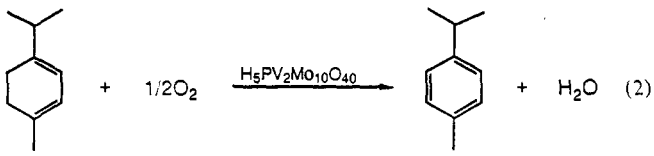


spectroscopic methods have been applied in order to gain a good understanding of and further insight into aerobic oxidative dehydrogenations catalyzed by heteropolyoxovanadomolybdates.

## Results and Discussion

**Kinetics of α-Terpinene Oxidative Dehydrogenation.** The first stage in the investigation of $H_5PV_2Mo_{10}O_{40}$-catalyzed oxidative dehydrogenation of α-terpinene was to verify the expected 2/1 α-terpinene/dioxygen stoichiometry of the reaction. This was done so that any reaction of α-terpinene related to nonoxidative transformations such as the acid-catalyzed disproportionation to *p*-cymene and *p*-menthene or polymerization could be ruled out.[30] Thus, in a typical oxidation, 3 mmol of α-terpinene and 1.25 mol % $H_5PV_2Mo_{10}O_{40}$ were dissolved in 3 mL of acetonitrile and the solution was kept at 25 °C under an oxygen atmosphere by using a gas buret. The formation of *p*-cymene and disappearance of α-terpinene were monitored by GLC, whereas the amount of dioxygen used was measured volumetrically (constant pressure) with the gas buret. Plots of the formation of *p*-cymene and the consumption of dioxygen as functions of time (Figure 2) show a ratio of slopes of 1.95, indicating that the expected 2/1 α-terpinene/dioxygen stoichiometry is correct. Additionally, the linearity ($r$ = 0.99) of the *p*-cymene (also α-terpinene) concentration as a function of time shows that the reaction is zero order in the α-terpinene substrate with an observed rate constant, $k_{obs}$, of 6.58 × $10^{-5}$ mol/(L s) at the given conditions (1.25 mol % $H_5PV_2Mo_{10}O_{40}$, 25 °C, $P_{dioxygen}$ = 0.94 atm).

Further experiments were performed to find the reaction orders in the remaining constituents of the reaction, the dioxygen pressure, and $H_5PV_2Mo_{10}O_{40}$ concentration. In order to find the reaction order in dioxygen, oxidations were run with pure dioxygen at constant atmospheric or subatmospheric pressures (0.18–1.0 atm), whereas to determine the catalyst concentration, oxidations were run at various catalyst concentrations (0.005–0.015 M); the conversion of α-terpinene was measured by GLC. At constant catalyst concentration and dioxygen pressure the zero-order rate

(30) Accrombessy, G.; Blanchard, M.; Petit, F.; Germain, J. E. *Bull. Soc. Chim. Fr.* **1974**, 705.

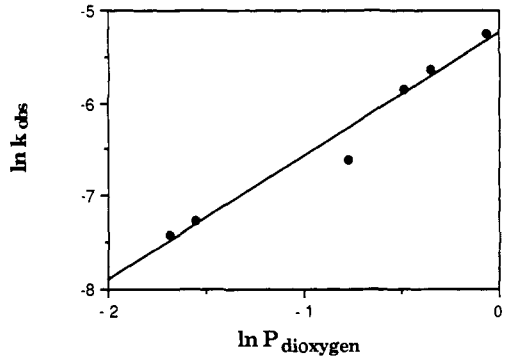


**Figure 3.** Plot of the observed rate constant of α-terpinene oxidation as a function of the dioxygen pressure. Reaction conditions: 3 mmol of α-terpinene and 0.0375 mmol of $H_5PV_2Mo_{10}O_{40}$ in 3 mL of acetonitrile at various dioxygen pressures at 25 °C.

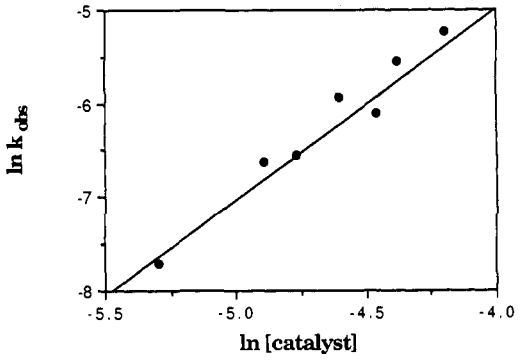


**Figure 4.** Plot of the observed rate constant of α-terpinene oxidation as a function of the catalyst concentration. Reaction conditions: 3 mmol of α-terpinene and various amounts of $H_5PV_2Mo_{10}O_{40}$ in 3 mL of acetonitrile at a dioxygen pressure of 0.94 atm at 25 °C.

constant, $k_{obs}$, may be described as follows: or

$$Cat_{red} + 2H^+ + \tfrac{1}{2}O_2 \rightarrow Cat_{ox} + H_2O \quad (1)$$

$$k_{obs} = k'[H_5PV_2Mo_{10}O_{40}]^m \qquad k' = k(P_{dioxygen})^n \quad (3)$$

Logarithmic plots of ln $k_{obs}$ vs ln $P_{dioxygen}$ (Figure 3) and ln $k_{obs}$ vs ln $[H_5PV_2Mo_{10}O_{40}]$ (Figure 4) enable direct calculation of the reaction orders in dioxygen and $H_5PV_2Mo_{10}O_{40}$, $n$ and $m$, respectively. Thus, we found that $n$ = 1.3 ($r$ = 0.98) and $m$ = 2.0 ($r$ = 0.98), and therefore the full rate equation may be given by eq 4. The empirical noninteger order of reaction in dioxygen

$$\text{rate} = k[H_5PV_2Mo_{10}O_{40}]^2[\alpha\text{-terpinene}]^0(P_{dioxygen})^{1.3} \quad (4)$$

pressure may be explained as follows. Since the reaction occurs in the liquid phase but the dioxygen pressure is a gas-phase measurement, it is probable that the liquid-phase dioxygen concentration is not linearly proportional to the external pressure, as predicated by Henry's law. This deviation from ideality could be explained by (a) mass-transfer limitations or (b) increased solubility at higher pressures due to increased dioxygen dissolution by complexation to the catalyst, for example. In the former case, the liquid-phase oxygen concentration would be lower at higher pressures than suggested by the gas-phase pressure and the true reaction order in dioxygen would be greater than 1.3, whereas, in the latter case, the liquid-phase dioxygen concentration would be higher and the true reaction order would be lower than 1.3.

Since direct measurement of the liquid oxygen concentration with an oxygen electrode was not possible due to the nature of the solvent, indirect methods were sought to differentiate between mass-transfer limitations and increased solubility by complexation. First, several oxidations were run at different stirring regimes: without stirring, at medium magnetic stirring, and with vigorous stirring. The observed rate constants in all cases did not differ significantly ($k_{obs}$ = (6.75 ± 0.50) × $10^{-5}$ mol/(L s) at 1.25 mol

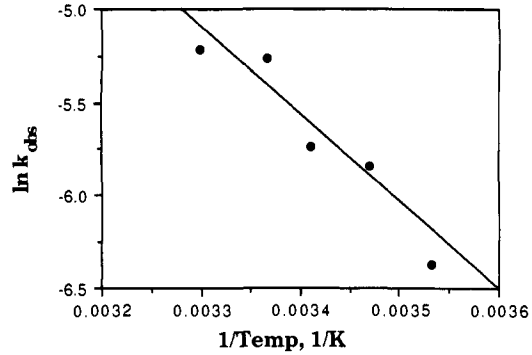


**Figure 5.** Plot of the observed rate constant of $\alpha$-terpinene oxidation as a function of the reaction temperature. Reaction conditions: 3 mmol of $\alpha$-terpinene and 0.0375 mmol of $H_5PV_2Mo_{10}O_{40}$ in 3 mL of acetonitrile at a dioxygen pressure of 0.94 atm at various temperatures.

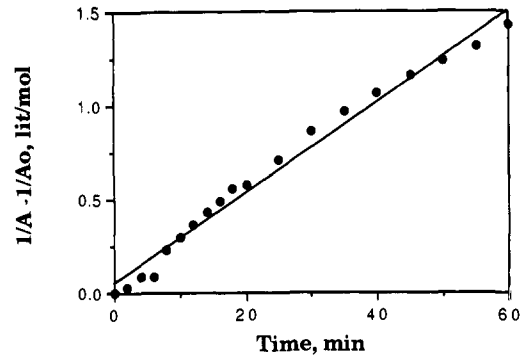


**Figure 6.** Reaction profile (second-order plot) of the reoxidation of an $\alpha$-terpinene-reduced $H_5PV_2Mo_{10}O_{40}$ catalyst. Reaction conditions: A 20 mM solution of $H_5PV_2Mo_{10}O_{40}$ in acetonitrile was reduced by 2 equiv of $\alpha$-terpinene and reoxidized under a 0.95-atm dioxygen pressure at 25 °C.

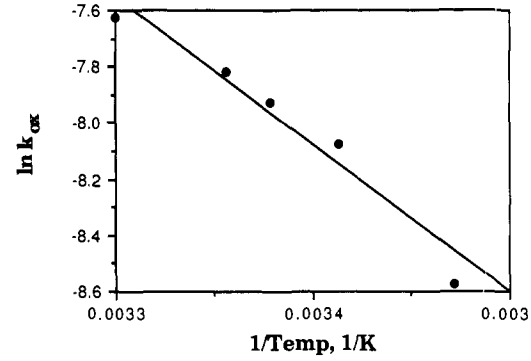


**Figure 7.** Plot of the observed rate constant of the catalyst reoxidation reaction as a function of temperature. Reaction conditions: A 20 mM solution of $H_5PV_2Mo_{10}O_{40}$ in acetonitrile was reduced by 2 equiv of $\alpha$-terpinene and reoxidized under a 0.95-atm dioxygen pressure at various temperatures.

% $H_5PV_2Mo_{10}O_{40}$, 25 °C, $P_{dioxygen}$ = 0.94 atm), indicating that mass transfer of dioxygen from the gas phase into the liquid phase was not an important factor. Further insight may also be gained by calculation of the activation energy from an Arrhenius plot (Figure 5). The computed activation energy was 10.1 kcal/mol ($r$ = 0.96; $\Delta H^{\ddagger}_{298}$ = 9.51 kcal/mol and $\Delta S^{\ddagger}_{298}$ = −27.2 eu), which is a low but appropriate value for a reaction where the rate-determining step is the chemical reaction.[31] Diffusion or mass transfer limited reactions generally have activation energies of 3–5 kcal/mol. One may also note that the value of $\Delta S^{\ddagger}_{298}$ is also indicative of a highly ordered transition state in the rate-determining step of the reaction. One may therefore conclude that the noninteger value for the reaction order in dioxygen pressure is due to increased solubility as a function of pressure and that the true reaction order for dioxygen in the liquid phase is less than 1.3 and most likely first order, suggesting the full rate equation shown in eq 5. Another source, suggested by a reviewer, of the

$$\text{rate} = k[H_5PV_2Mo_{10}O_{40}]^2[\alpha\text{-terpinene}]^0[\text{dioxygen}]^1 \quad (5)$$

fractional order in dioxygen could be a mixture of first- and second-order processes with similar rates. Although such a possibility cannot be refuted, the probability of interaction of two dioxygen molecules in a rate-determining step is, in our opinion, only very small and unprecedented.

According to a simplified reaction scheme (eq 6), the complete catalytic oxidation reaction may be divided into two separate

$$SH_2 + PV^{V}_2Mo_{10}O_{40}^{5-} \rightarrow S + PV^{IV}_2Mo_{10}O_{40}^{7-} + 2H^+$$
$$PV^{IV}_2Mo_{10}O_{40}^{7-} + 2H^+ + \tfrac{1}{2}O_2 \rightarrow PV^{V}_2Mo_{10}O_{40}^{5-} + H_2O \quad (6)$$

reactions: an $\alpha$-terpinene oxidative dehydrogenation or catalyst reduction step and a catalyst reoxidation step. We decided to investigate the kinetics of each of these stages independently by following the reduction and reoxidation of the $H_5PV_2Mo_{10}O_{40}$ catalyst upon addition of 1 equiv (stoichiometric reaction) of $\alpha$-terpinene to a 1.5 mM solution of $H_5PV_2Mo_{10}O_{40}$ in acetonitrile. The redox reaction of the catalyst is easily followed by visible absorption spectrometry at 600–750 nm due to the characteristic heteropoly blue color of the reduced $PV_2Mo_{10}O_{40}$ species. The catalyst reduction step is a fast reaction with a half-life, $\tau_{1/2}$, of ~3 s and is first order in the formation of the reduced catalyst ($k_{red}$ = 0.16 ± 0.02 $s^{-1}$ at 20 °C for a 1.5 mM $H_5PV_2Mo_{10}O_{40}$ solution). The catalyst reoxidation reaction was measured in more concentrated solutions (20 mM), similar to those used in the complete catalytic oxidation. The catalyst reoxidation is second order in the $H_5PV_2Mo_{10}O_{40}$ catalyst (Figure 6) and is slower than the catalyst reduction by approximately 3 orders of magnitude ($\tau_{1/2}$ = 370 s, $k_{ox}$ = 4.02 × $10^{-4}$ L/(mol s) ($r$ = 0.99) at 25 °C, and $P_{dioxygen}$ = 0.19 atm for a 20 mM solution). It is interesting to note that the computed time required to complete half of one turnover in the catalytic oxidative dehydrogenation under similar conditions[32] is ~390 s, comparing well with the half-life of the catalyst reoxidation reaction. The activation energy of the catalyst reoxidation reaction from an Arrhenius plot (Figure 7) was calculated to be 10.4 kcal/mol ($r$ = 0.99; $\Delta H^{\ddagger}_{298}$ = 9.81 kcal/mol and $\Delta S^{\ddagger}_{298}$ = −29.6 eu).

It seemed obvious at this point that the reoxidation of the catalyst with dioxygen was the reaction's rate-determining step, since (a) the oxidation in its entirety was zero order in $\alpha$-terpinene, (b) the catalyst reoxidation was significantly slower than the catalyst reduction, (c) the reaction was second order in the $H_5PV_2Mo_{10}O_{40}$ catalyst for both the catalytic oxidative dehydrogenation and catalyst reoxidation with similar times required for half of one turnover, and (d) the activation energy for the oxidative dehydrogenation was the same as that for the catalyst reoxidation. At this stage, from only a kinetic point of view, a simple mechanism can be formulated whereby the $\alpha$-terpinene substrate is dehydrogenated to *p*-cymene in the reaction's first step, forming a reduced heteropoly blue. The catalyst reoxidation rate-determining step would then require interaction of two reduced molecules and two protons with dioxygen, yielding an oxidized catalyst and water.

**Mechanism of $\alpha$-Terpinene Oxidative Dehydrogenation.** In order to gain more insight into the mechanism of the catalytic dehydrogenation reactions, further investigations were initiated. Again, the catalytic oxidation was divided into catalyst reduction and reoxidation steps. Dealing first with the catalyst reduction, we expected, according to eq 6, that a simple catalyst–substrate irreversible reaction of a 1/1 stoichiometry would occur entailing a two-electron reduction of the $H_5PV_2Mo_{10}O_{40}$ catalyst[33] coin-

(31) Satterfield, C. N. *Mass Transfer in Heterogeneous Catalysis*; MIT Press: Cambridge, MA, 1970.

(32) The computation was performed by interpolation to the appropriate conditions using Figures 3 and 4.

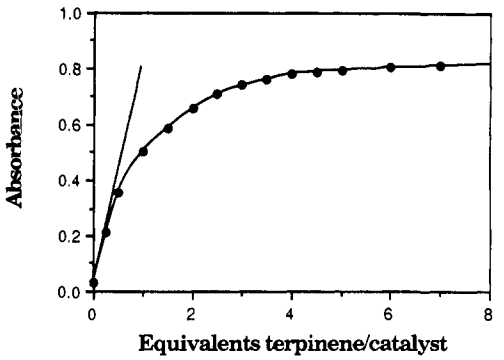


**Figure 8.** Absorption at 750 nm of an 8 mM solution of $PV_2Mo_{10}O_{40}$ in acetonitrile after addition of α-terpinene.

cident with an α-terpinene to *p*-cymene two-electron oxidation. However, upon addition of increasing amounts of α-terpinene to a $H_5PV_2Mo_{10}O_{40}$ solution, measurement of the heteropoly blue absorption at 750 nm (Figure 8) shows unexpected behavior. Whereas an irreversible redox reaction would require a linear increase in absorption upon addition of α-terpinene until a maximum was reached at the required α-terpinene/catalyst stoichiometry, one finds instead an asymptotic behavior indicative of a reversible or equilibrium reaction between substrate and catalyst. Since, from the initial slope of the curve, the expected 1/1 α-terpinene/catalyst ratio may be deduced, the initial redox stage of the reaction could be reformulated as an equilibrium reaction (eq 7). Simple free energy calculations ($\Delta G°_f = \sim -44$ kcal/mol) using known literature values[34] show, however, that the reverse, right to left, reaction as given in eq 7 is impossible. This forces a preliminary conclusion that α-terpinene and $H_5PV_2Mo_{10}O_{40}$ react reversibly to form a higher energy intermediate. Such an intermediate may be described as an electron-transfer complex consisting of a reduced heteropolyanion attached to an oxidized cation radical of α-terpinene (eq 8). The α-terpinene cation radical in this intermediate may then undergo deprotonation, forming an α-terpinene radical complexed to a protonated and reduced catalyst (eq 9). It may be noted that association complexes between organic molecules and heteropolyanions have been observed in the past for the interactions of 1-propanol with $H_3PW_{12}O_{40}$[5a] and tetramethylurea with $H_3PMo_{12}O_{40}$.[35] Further, it may be noted that the α-terpinene$^{\bullet}$–$H_6PV^{V}V^{IV}Mo_{10}O_{40}$ complex could conceivably be formed directly from α-terpinene and $H_5PV_2Mo_{10}O_{40}$ by hydrogen atom transfer. However, in reactions such as the oxidative dehydrodimerization of dialkylphenols[22] (eq 10), we have observed that the oxidation potential of $H_5PV_2Mo_{10}O_{40}$ ($E°$ = 0.79 V by cyclic voltammetry) is strongly correlated with the reactivity and oxidation potential of the substrate phenol (Table I). This correlation leads us, in the general case, to prefer an electron-transfer mechanism with a cation radical intermediate rather than a hydrogen-transfer mechanism.

$$\text{α-terpinene} + H_5PV^{V}{}_2Mo_{10}O_{40} \rightleftarrows p\text{-cymene} + H_7PV^{IV}{}_2Mo_{10}O_{40} \quad (7)$$

$$\text{α-terpinene} + H_5PV_2Mo_{10}O_{40} \rightleftarrows \text{α-terpinene}^{\bullet+}\text{–}H_5PV^{V}V^{IV}Mo_{10}O_{40} \quad (8)$$

$$\text{α-terpinene}^{\bullet+}\text{–}H_5PV^{V}V^{IV}Mo_{10}O_{40} \rightleftarrows \text{α-terpinene}^{\bullet}\text{–}H_6PV^{V}V^{IV}Mo_{10}O_{40} \quad (9)$$

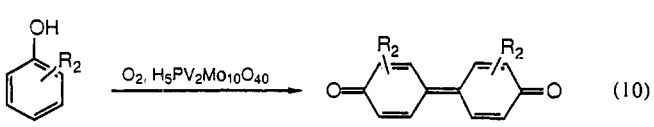


(10)

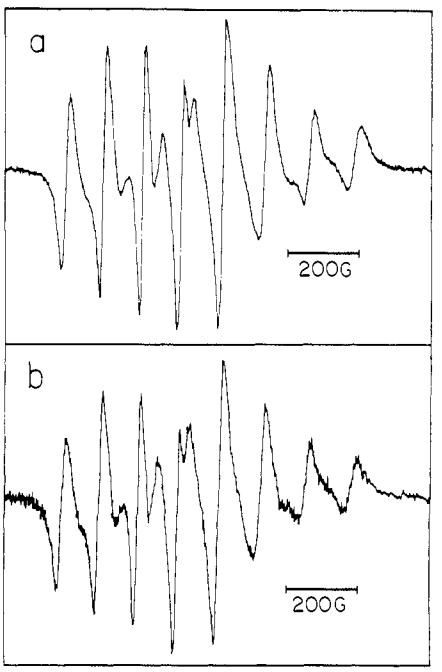


**Figure 9.** ESR spectra of a 20 mM solution of $PV_2Mo_{10}O_{40}$ in acetonitrile after (a) addition of 1 equiv of α-terpinene and (b) addition of 10 equiv of α-terpinene. Microwave frequency = 9.41 GHz, microwave power = 5 mW, and modulation amplitude = 1 G at ambient temperature. Receiver gain: (a) $2.5 \times 10^3$; (b) $5 \times 10^3$.

**Table I.** Oxidation of Alkylated Phenols to Diphenoquinones Catalyzed by $H_5PV_2Mo_{10}O_{40}$[a]

| substrate | rel conversn[b] | oxidn pot., $E°$ (V) |
|---|---|---|
| 2,6-di-*tert*-butylphenol | 1.00 | 0.68 |
| 2,6-dimethylphenol | 0.75 | 0.76 |
| 2,5-dimethylphenol | 0.32 | 0.82 |
| 3,5-dimethylphenol | 0.00 | 0.86 |

[a] Reaction conditions: 1 mmol of substrate, 0.02 mmol of $H_5PV_2Mo_{10}O_{40}$, 20 mL of ethanol, 1 atm of dioxygen, 60 °C, 4 h. [b] Conversions were computed by HPLC and are given relative to 2,6-di-*tert*-butylphenol.

At this point, direct and more concrete evidence was sought for the existence of the stipulated electron-transfer intermediate. The room-temperature ESR spectra of a 20 mM $H_5PV_2Mo_{10}O_{40}$ acetonitrile solution after addition of 1 equiv of α-terpinene is shown in Figure 9a. The spectrum is attributed to a one-electron-reduced $PV^{V}V^{IV}Mo_{10}O_{40}^{6-}$ species (previously prepared by controlled-potential electrolysis[36]) and is a combination ($g$ = 1.98) of an 8-line spectrum ($a$ = 108 G) (from $PV^{V}V^{IV}Mo_{10}O_{40}^{6-}$ isomers with nonvicinal vanadium atoms) and a 15-line spectrum ($a$ = 50 G) (from $PV^{V}V^{IV}Mo_{10}O_{40}^{6-}$ isomers with vicinal vanadium atoms).[36] Addition of an excess of 10 equiv of α-terpinene (Figure 9b) causes an expected approximately 2-fold reduction in the intensity of the ESR spectrum; however, it remains the same combined 8- and 15-line spectrum. The appearance of only a 15-line spectrum of reduced intensity attributed in the past[36] to

(33) In the past, we[20] and others had generally assumed that such an irreversible reaction takes place.

(34) $\Delta G°_f$ of the catalyst reduction was taken from cyclic voltammetry measurements ($E°$ = 0.78 V), and $\Delta G°_f$ of the α-terpinene to *p*-cymene transformation was computed from the information available on the analogous 1,3-cyclohexadiene to benzene reaction. (a) Stull, D. R.; Westrun, E. F.; Sinke, G. C. *The Chemical Thermodynamics of Organic Compounds*; Wiley: New York, 1969; p 367. (b) Dorofeeva, O. V.; Gurvich, L. V.; Jorish, V. S. *J. Phys. Chem. Ref. Data* **1986**, *15*, 437.

(35) (a) Hill, C. L.; Renneke, R. F.; Williamson, M. M. *J. Chem. Soc., Chem. Commun.* **1986**, 1747. (b) Hill, C. L.; Bouchard, D. A.; Kadkhodayan, M.; Williamson, M. M.; Schmidt, J. A.; Hilinski, E. F. *J. Am. Chem. Soc.* **1988**, *110*, 5471.

(36) (a) Pope, M. T.; O'Donnell, S. E.; Prados, R. A. *J. Chem. Soc., Chem. Commun.* **1975**, 22. (b) Pope, M. T.; O'Donnell, S. E.; Prados, R. A. In *Inorganic Compounds with Unusual Properties*; King, R. B., Ed.; American Chemical Society: Washington, DC, 1976; p 85.

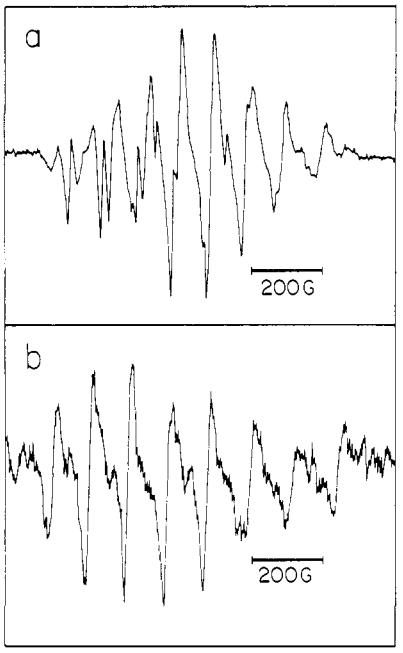


**Figure 10.** ESR spectra of $PV_2Mo_{10}O_{40}$ solutions in acetonitrile after addition of 2-methyl-2-nitrosopropane and (a) $\alpha$-terpinene or (b) $Fe^{II}SO_4$. Microwave frequency = 9.41 GHz, microwave power = 5 mW, and modulation amplitude = 1 G at ambient temperature. Receiver gain: (a) $10 \times 10^3$; (b) $10 \times 10^4$.

the two-electron-reduced $PV^{IV}{}_2Mo_{10}O_{40}{}^{7-}$ species was not observed. Thus, according to the ESR spectra, a two-electron-reduced $PV^{IV}{}_2Mo_{10}O_{40}{}^{7-}$ heteropolyanion is *not* formed upon addition of excess $\alpha$-terpinene. This finding supports the hypothesis whereby an electron-transfer complex, $\alpha$-terpinene$^{\bullet+}$–$H_5PV^{V}V^{IV}Mo_{10}O_{40}$, and then a stable (the ESR spectrum is unchanged after 6 h) $\alpha$-terpinene$^{\bullet}$–$H_6PV^{V}V^{IV}Mo_{10}O_{40}$ complex are formed in the initial interaction between $\alpha$-terpinene and the heteropolyanion catalyst.

Further addition of a 2-methyl-2-nitrosopropane spin trap to a 10 mM 3/1 $\alpha$-terpinene/catalyst solution resulted in the formation of a complex ESR spectrum (Figure 10a) containing attributes of the original $PV^{V}V^{IV}Mo_{10}O_{40}{}^{6-}$ spectrum and additional spectral lines apparently centered at about $g = 2.05$. A control experiment (at lower concentrations due to solubility considerations) (Figure 10b) where the spin trap was added to a $PV^{V}V^{IV}Mo_{10}O_{40}{}^{6-}$ compound prepared by reduction of $PV_2Mo_{10}O_{40}{}^{5-}$ by the known one-electron reductant Fe(II)[37] yielded only the typical $PV^{V}V^{IV}Mo_{10}O_{40}{}^{6-}$ ESR spectrum. Therefore, one may conclude that the additional spectral lines observed in Figure 10a are the result of a spin trap of an organic radical, presumably the stipulated $\alpha$-terpinene radical heteropolyanion species.

After formation of the relatively stable intermediate electron-transfer complex, one remains with the question of how the reaction proceeds. One possibility is that the intermediate undergoes diassociation to a free radical and a reduced heteropolyanion (eq 11).

$$\alpha\text{-terpinene}^{\bullet}\text{–}H_6PV^{V}V^{IV}Mo_{10}O_{40} \rightleftarrows \alpha\text{-terpinene}^{\bullet} + H_6PV^{V}V^{IV}Mo_{10}O_{40} \quad (11)$$

The absence of any oxygenated products formed by diffusion-controlled allylic dioxygen substitution or vinylic addition reactions tends to rule out the formation of a free radical. In fact, in previous synthetic work performed in the study of the oxidation of benzyl alcohol to benzaldehyde, we observed that no benzoic acid is formed due to the suppression of free radical autoxidation.[21] In the present study, we have additionally tested the suppression of another common autoxidation: that of tetralin in the presence of $H_5PV_2Mo_{10}O_{40}$ (eq 12). A 2 M solution of tetralin in acetonitrile was stirred and kept under a 1-atm dioxygen atmosphere for 10 h at 70 °C. In the absence of any catalyst, a 45.3% conversion to tetralin hydroperoxide was observed. On the other hand, the same reaction with only 0.5 mol % $H_5PV_2Mo_{10}O_{40}$ yields no oxidation product even after 24 h. Keeping in mind the high autoxidizability of benzaldehyde and tetralin vs that of $\alpha$-terpinene,[38] the suppression of the autoxidation of benzaldehyde and tetralin by the heteropolyanion catalyst would seem to indicate that any free radical initially formed by a thermal reaction is immediately quenched or bound to the catalyst. Similarly, one may conclude for the $\alpha$-terpinene case that no free radical is present and that the disassociation reaction described in eq 11 is not part of the reaction pathway. The antioxidant type behavior of the $H_5PV_2Mo_{10}O_{40}$ compound deserves some additional comment, especially since the 2-methyl-2-nitrosopropane spin trap does show interaction with a bound $\alpha$-terpinene radical species, whereas the diffusion-controlled reaction of an organic radical with dioxygen is suppressed. We surmise that this phenomenon is best explained by the reaction of dioxygen with the reduced heteropolyanion instead of the bound $\alpha$-terpinene moiety in a manner which will be elaborated upon below, whereas the spin trap does not react with the reduced heteropolyanion (Figure 10b).

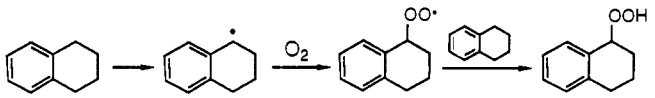

(12)

Another possible fate of the $\alpha$-terpinene–heteropolyanion complex is either fast electron (carbocation intermediate) and proton transfer or possibly hydrogen atom transfer.[39] In both cases, a doubly protonated reduced heteropolyanion and *p*-cymene are generated through a bound intermediate, followed by the rate-limiting reoxidation of the reduced catalyst by dioxygen (eqs 13 and 14). This possibility is supported by the observed reaction

$$\alpha\text{-terpinene}^{\bullet}\text{–}H_6PV^{V}V^{IV}Mo_{10}O_{40} \rightleftarrows p\text{-cymene–}H_7PV^{IV}{}_2Mo_{10}O_{40} \rightleftarrows p\text{-cymene} + H_7PV^{IV}{}_2Mo_{10}O_{40} \quad (13)$$

$$2H_7PV^{IV}{}_2Mo_{10}O_{40} + O_2 \rightarrow 2H_5PV^{V}{}_2Mo_{10}O_{40} + 2H_2O \quad (14)$$

kinetics (zero order in $\alpha$-terpinene, second order in $H_5PV^{V}{}_2Mo_{10}O_{40}$, and first order in dioxygen). Even though the ESR spectra show no doubly reduced heteropolyanion, a small but fast equilibrium formation of *p*-cymene and $H_7PV^{IV}{}_2Mo_{10}O_{40}$ is still definitely possible. Alternatively, dioxygen could conceivably react directly with $\alpha$-terpinene$^{\bullet}$–$H_6PV^{V}V^{IV}Mo_{10}O_{40}$ in a 1/2 stoichiometry, yielding *p*-cymene, water, and the oxidized catalyst. In our opinion, the probability of such a reaction is very small, considering the number of transformations which must occur simultaneously, and we prefer the reaction pathway of eqs 13 and 14.

The last part of the research into the reaction mechanism dealt with the catalyst reoxidation step. For photocatalytic dehydrogenations, there has only very recently been a study reported[40] whereas, for thermal dehydrogenations, there is only scant information in the literature on this subject, all of which deals exclusively with aqueous solutions. The general approach[41] has been to postulate a four-electron reduction of dioxygen to water by a $PV^{IV}{}_4Mo_8O_{40}{}^{11-}$ species formed by disproportionation re-

(37) Chernysova, Y. V.; Kuznetsova, L. I.; Matveev, K. I. *React. Kinet. Catal. Lett.* **1988**, *37*, 221.

(38) Howard, J. A. *Adv. Free-Radical Chem.* **1972**, *4*, 49.

(39) It is difficult in this case to differentiate between electron-transfer and atom-transfer mechanisms, because in attempted oxidations with substrates such as fluorene, which would tend to yield stable carbocation intermediates, the carbocation alternatively could also be formed by acid catalysis.

(40) Hiskia, A.; Papaconstantinou, E. *Inorg. Chem.* **1992**, *31*, 163.

(41) Kuznetsova, L. I.; Maksimovskaya, R. I.; Matveev, K. I. *Inorg. Chim. Acta* **1986**, *121*, 137.

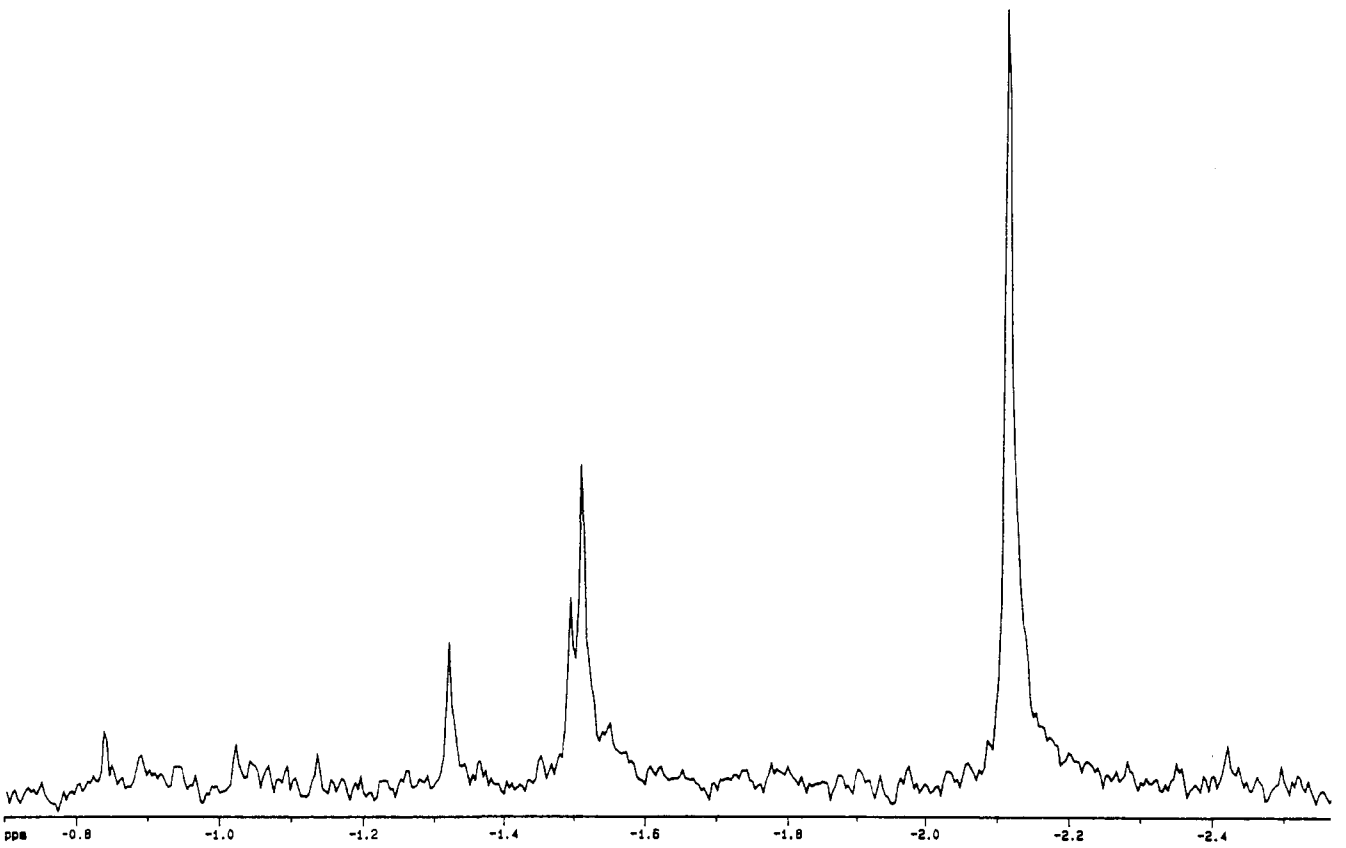


**Figure 11.** $^{31}P$ NMR spectrum of 20 mM $H_5PV_2Mo_{10}O_{40}$ in acetonitrile after reaction with 10 equiv of $\alpha$-terpinene.

actions of phosphovanadomolybdates containing fewer vanadium atoms. We have sought to reevaluate this question for reactions which occur in organic media.

First, we wished to determine if the dioxygen is directly reduced to water or whether free superoxide or peroxide intermediates are formed. The fact that autoxidations are suppressed by $PV_nMo_{12-n}O_{40}$ compounds seems a priori to preclude the formation of a superoxide intermediate. Furthermore, the oxidation potential of the heteropolyanion/dioxygen–superoxide pair shows that the reduction of $H_5PV^V_2Mo_{10}O_{40}$ by superoxide is the thermodynamically favored reaction. In fact, addition of potassium superoxide to an acetonitrile solution of $H_5PV^V_2Mo_{10}O_{40}$ causes immediate reduction of the heteropolyanion coupled with dioxygen formation (eq 15), decisive proof that superoxide is not a reaction intermediate.

$$H_5PV^V_2Mo_{10}O_{40} + KO_2 \rightarrow KH_5PV^VV^{IV}Mo_{10}O_{40} + O_2 \quad (15)$$

Another reoxidation mechanism which could be formulated takes into account a two-electron reduction of dioxygen. In this case, dioxygen would react with a doubly reduced and protonated heteropolyanion, forming hydrogen peroxide (eq 16). The hydrogen peroxide thus formed could then reoxidize another reduced heteropolyanion species in an additional two-electron process. In order to test this hypothesis, 1 equiv of 30% hydrogen peroxide was added to a 20 mM acetonitrile solution of 1/1 $\alpha$-terpinene and $H_5PV_2Mo_{10}O_{40}$ at room temperature. After 1 h, the reaction mixture was analyzed by GLC and found to contain five major oxygenated products but *no* *p*-cymene. The oxygenated products as determined by GC–MS are all monoepoxides (the Keggin compounds are known epoxidation catalysts with hydrogen peroxide[9]) formed through epoxidation of $\alpha$-terpinene and other isomeric endodienes. It therefore seems probable that hydrogen peroxide is not formed as an intermediate and the reoxidation of the catalyst proceeds through a direct four-electron reduction of dioxygen to water.

$$H_7PV^{IV}_2Mo_{10}O_{40} + O_2 \rightarrow H_5PV^V_2Mo_{10}O_{40} + H_2O_2 \quad (16)$$

**Table II.** $^{31}P$ NMR Chemical Shifts of Various $H_{3+n}PV_nMo_{12-n}O_{40}$ Heteropolyanions[a]

| heteropoly-anion compd | chemical shift (ppm) |
|---|---|
| $H_3PMo_{12}O_{40}$ | −2.49 |
| $H_4PV_1Mo_{11}O_{40}$ | −2.24 |
| $H_5PV_2Mo_{10}O_{40}$ | −2.11 (5), −1.51 (2), −1.49 (1), −1.32 (1) |
| $H_6PV_3Mo_9O_{40}$ | −2.19, −2.07, −1.45, −1.42, −1.39, −1.32, −1.16, −1.09, 1.07 |

[a] Solutions were 20 mM heteropolyanion in 1/4 $CD_3CN/CH_3CN$; spectra were taken at ambient temperature, and the chemical shifts given are upfield from the external standard ($H_3PO_4$).

Although the reaction kinetics clearly indicate a 2/1 catalyst to dioxygen ratio in the rate-determining step, which is easily rationalized by a reaction step as represented in eq 14, we wanted clear evidence that there was no catalyst disproportionation as had been claimed for aqueous solutions. A series of $H_{3+n}PV_nMo_{12-n}O_{40}$ ($n$ = 0–3) heteropolyanions were synthesized and their $^{31}P$ NMR spectra taken in acetonitrile (Table II and Figure 11).[42] As can be seen, it is easy to differentiate between the various compounds. An additional $^{31}P$ NMR spectrum was taken of a reaction mixture in which 10 equiv of $\alpha$-terpinene was added to a 20 mM solution of $H_5PV_2Mo_{10}O_{40}$ in acetonitrile. The reaction was kept under dioxygen for 5 h to allow complete conversion and reoxidation of the catalyst. The resulting $^{31}P$ NMR spectrum was in all respects identical to the spectrum of $H_5PV_2Mo_{10}O_{40}$, which had not undergone reaction and whose spectrum contains no peaks attributable to other $H_{3+n}PV_nMo_{12-n}O_{40}$ compounds or other phosphorus-containing compounds. This result seems to indicate that there is no *significant* fragmentation (eq 17) of the catalyst during the reaction because the formation of

$$PV^VV^{IV}Mo_{10}O_{40}^{6-} \rightarrow PV^VMo_{10}O_{39}^{8-} + V^{IV}O^{2+} \quad (17)$$

(42) The relative areas of the peaks seem to indicate that either all catalyst stereoisomers are not present or they are not present in their expected statistical distribution.

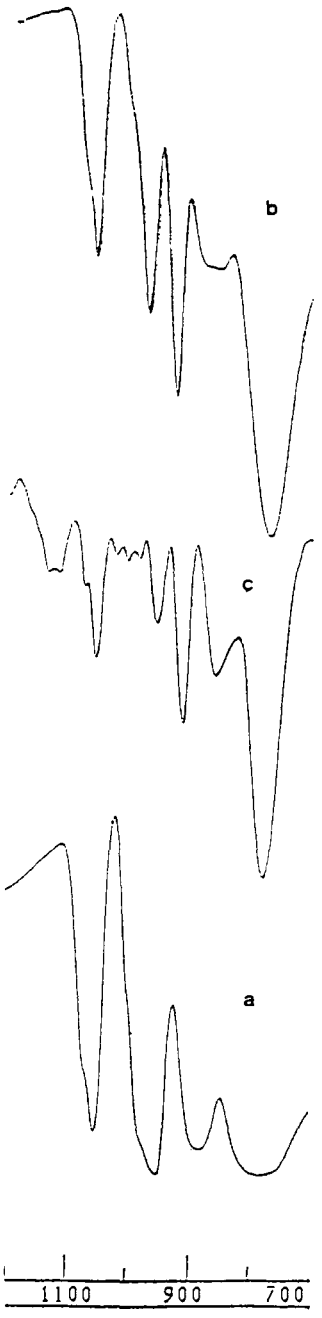


**Figure 12.** IR spectra of (a) $H_5PV_2Mo_{10}O_{40}$ (b) $H_5PV_2Mo_{10}O_{40}$ treated with $H_2{}^{18}O$, and (c) $H_2{}^{18}O$-treated catalyst after reaction with $\alpha$-terpinene.

the unstable lacunary species $PVMo_{11}O_{39}$ would invariably yield some disproportionation products (e.g. $PVMo_{11}O_{40}$ and $PV_3Mo_9O_{40}$) and/or lead to catalyst destruction and products such as $PO_4^{3-}$. Formation of fragments such as $VO_2^+$ or $VO^{2+}$ with potential catalytic activity at low concentrations cannot be, of course, entirely excluded due to the limited sensitivity of the $^{31}P$ NMR method.

Since the reduction of dioxygen is a four-electron process, the heteropolyanion catalyst retains its composition throughout the reaction cycle, and the reaction is second order in the heteropolyanion catalyst and first order in dioxygen, a probable reaction mechanism calls for interaction of two molecules of $H_7PV^{IV}{}_2Mo_{10}O_{40}$ and dioxygen through an intermediate to yield water and the reoxidized catalyst (eq 18).

$$2H_7PV^{IV}{}_2Mo_{10}O_{40} + O_2 \rightarrow [H_7PV^{IV}{}_2Mo_{10}O_{40}{-}O_2{-}H_7PV^{IV}{}_2Mo_{10}O_{40}] \rightarrow 2H_5PV^{V}{}_2Mo_{10}O_{40} + 2H_2O \quad (18)$$

**Scheme I.** Mechanistic Scheme for the Oxidative Dehydrogenation of $\alpha$-Terpinene Catalyzed by the $H_5PV_2Mo_{10}O_{40}$ Heteropolyanion

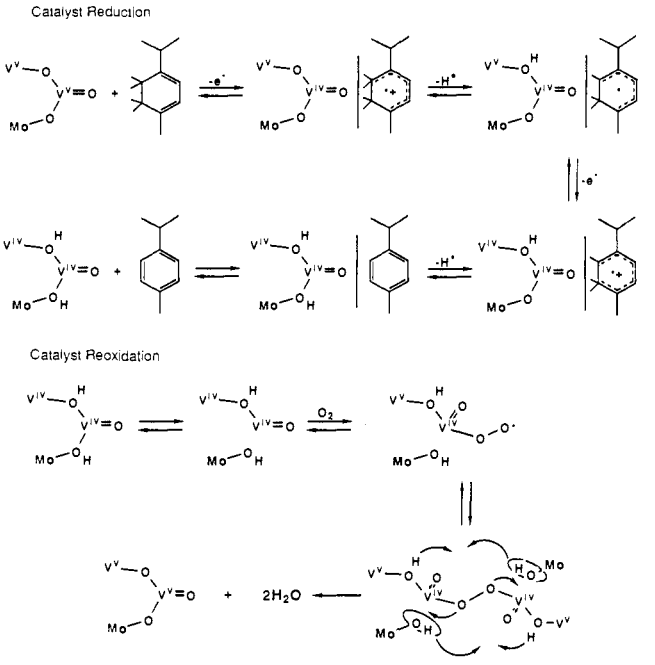


In order to obtain more information on the nature of the postulated intermediate, IR spectra were taken of the oxidized catalyst, $H_5PV^{V}{}_2Mo_{10}O_{40}$, of the same catalyst after treatment with $H_2{}^{18}O$, and of the $H_2{}^{18}O$-treated catalyst after addition and oxidation of 5 equiv of $\alpha$-terpinene in 1 atm of $^{16}O_2$ (Figure 12). The IR spectrum of the original catalyst (Figure 12a) has four peaks attributable[43] to the four different types of oxygen bonds, that is, P–$O_p$ (internal oxygen connecting P and M) at 1051 $cm^{-1}$, M–$O_t$ (terminal oxygen bonding to one M) at 958 $cm^{-1}$, M–$O_c$–M (corner-sharing oxygen connecting $M_3O_{13}$ units) at 883 $cm^{-1}$, and M–$O_e$–M (edge-sharing oxygen connecting M's) at 775 $cm^{-1}$. Treatment of the original catalyst with a large excess of $H_2{}^{18}O$ (see details in the Experimental Section) (Figure 12b) shows that the $O_t$ and $O_p$ oxygens were not replaced, the P–$O_p$ and M–$O_t$ peaks remaining at 1050 and 960 $cm^{-1}$, respectively. Likewise, surprisingly the M–$O_e$–M band remains at its former position (772 $cm^{-1}$), but is stronger and sharper than that of the original catalyst. Such phenomena have been observed in the past[43b] and are not due to isotope substitution. A new absorption band appears, however, at 917 $cm^{-1}$ instead of the peak at 883 $cm^{-1}$ and is assigned to a M–$^{18}O_c$–M band. The new catalyst, formally $H_5PV_2Mo_{10}{}^{18}O_{12}{}^{16}O_{28}$, was reacted with 5 equiv of $\alpha$-terpinene under $^{16}O_2$ in acetonitrile until the catalyst was completely reoxidized. The IR spectrum after evaporation of the solvent showed the reappearance of the M–$^{16}O_c$–M band. It is also important to note that (a) under nonreaction conditions the $^{18}O$-exchanged catalyst showed no change in the IR spectrum over a period of 3 days and (b) with 2.5 equiv of $O_2$ a maximum of 20% $^{18}O \rightarrow {}^{16}O$ replacement may be expected. It seems clear that the M–$O_c$–M bond is the weak link in the heteropolyanion structure. Additionally, it is apparent that, during the catalyst reduction by $\alpha$-terpinene, the M–$O_c$–M bond is weakened (see below) because on the one hand a large excess of $H_2{}^{18}O$ is needed for complete $^{16}O \rightarrow {}^{18}O$ transformation of the $O_c$ oxygen in the catalyst's original oxidized form but on the other hand only small amounts of $^{16}O_2$ under reaction conditions are required for the $^{18}O \rightarrow {}^{16}O$ reversion.

Taking into account the kinetic results and the information gained from the $^{31}P$ NMR and IR spectra, a possible catalyst reoxidation mechanism (as part of the entire reaction scheme,

(43) (a) Rocchicciolini-Deltcheff, C.; Thouvenot, R.; Franck, R. *Spectrochim. Acta* **1976**, *32A*, 587. (b) Rocchicciolini-Deltcheff, C.; Fournier, M.; Franck, R.; Thouvenot, R. *Inorg. Chem.* **1983**, *22*, 207.

Scheme I) may be suggested. First, the labile M–$O_c$–M bond is broken, induced perhaps by the binding of α-terpinene. Second, a μ-peroxo type intermediate complex is formed, possibly via a transient superoxo complex, by two heteropolyanion molecules and dioxygen. The O–O bond can then be broken, coupled with re-formation of the M–$O_c$–M bond and two molecules of water. The μ-peroxo type intermediate has been implicated in the past in vanadium and molybdenum oxidations.[44] Concerning the catalyst reoxidation scheme, it is worthwhile to point out some additional points. The mechanism as drawn shows $PV_2Mo_{10}O_{40}$ isomers where the two vanadium atoms are in proximity (the 1,2 and 1,6 isomers which statistically are 36.4% of the total[36b]) and protonation at the bridging oxygen atoms. While we do not claim that these are the only reactive isomers or protonation sites, it is reasonable to assume that these are the more reactive isomers and most likely protonation sites for several reasons. First, it has been shown that, for V–O–V type isomers, there is rapid electron exchange between the neighboring vanadium atoms whereas, in isomers of the V–O–M–O–V type, electrons are trapped on a single vanadium atom.[36b] Therefore, it seems probable that the reduction of dioxygen requiring two electrons from each heteropolyanion species would occur through the reduced isomers which would donate the electrons most efficiently; this means dioxygen would preferentially bind at vanadium centers in V–O–V type isomers. Unfortunately, the present unavailability of pure isomers prevents direct comparison of the catalytic efficiencies of the isomeric forms. Second, it has been shown both by computation[45] and by experiment[46] that protonation occurs at bridging oxygen atoms due to their higher electron density where the propensity for protonation decreases in the following order: V–O–V > V–O–Mo > Mo–O–Mo. As a final thought, it may be noted that much of the experimental evidence could lead to the conclusion that the μ-peroxo compound is the stable reaction intermediate instead of the α-terpinene$^{\bullet}$–$H_6PV^{V}V^{IV}Mo_{10}O_{40}$ complex. However, the spin trap experiment along with the fact that antiferromagnetic coupling of the μ-peroxo intermediate would result in no ESR signal leads us to prefer the delineated reaction scheme.

## Summary

An in depth investigation into a model oxidative dehydrogenation reaction of α-terpinene to *p*-cymene catalyzed by the $H_5PV_2Mo_{10}O_{40}$ heteropolyanion has shed new light on the mechanism of thermal oxidations catalyzed by this family of heteropolyanions, which due to their inherent stability show great future promise as durable catalysts. Oxidative dehydrogenations take place by formation of an intermediate catalyst–substrate electron-transfer complex. After completion of the substrate oxidation or catalyst reduction, the catalyst is reoxidized via a proposed μ-peroxo intermediate whereby the primary oxidant, molecular oxygen, undergoes a four-electron reduction to water. It is also quite possible that the catalyst reoxidation mechanism is valid for additional types of heteropolyanion-catalyzed reactions, especially the phosphotungstate-catalyzed photoactivated oxidative dehydrogenations.

## Experimental Section

**Materials and Instrumentation.** The α-terpinene was a commercial product (Hercules) of 95% purity by GLC and $^{13}C$ NMR spectroscopy containing about 4.5% *p*-cymene and about 0.5% additional unidentified monoterpene impurity. The $H_5PV_2Mo_{10}O_{40}$ catalyst was prepared by the standard technique[47] and used as the hydrate unless specifically stated otherwise. $H_2{}^{18}O$ was an Alfa product with 90% isotope enrichment. All other compounds were analytical reagents and were used without treatment. Gas–liquid chromatography (GLC) was conducted with a Hewlett Packard 5890 instrument equipped with an FID detector and using helium as the carrier gas. Peaks were quantified by an HP-3396A integrator after calibration with known amounts of α-terpinene and *p*-cymene. The column used was a 10-m (length) × 530-μm (i.d.) cross-linked FFAP at a column temperature of 50 °C. Retention times were 1.3 min for α-terpinene and 2.4 min for *p*-cymene. Ultraviolet and visible spectra were obtained with a Hewlett Packard 8452A diode-array spectrometer equipped with a temperature bath and stirrer. Electron spin resonance spectra were taken on a Varian E-12 spectrometer at room temperature in a quartz flat cell. Phosphorus-31 NMR spectra were recorded with a Bruker AMX400 spectrometer at 161.98 MHz using a deuterium lock ($CD_3CN$) and $H_3PO_4$ as an external standard. Infrared spectra were measured on an Analect RFX-30 FTIR instrument. GC–MS measurements were performed on a Hewlett Packard 5790A instrument.

**Oxidative Dehydrogenation of α-Terpinene.** In a typical experiment, 0.03 mmol of $H_5PV_2Mo_{10}O_{40}$ was dissolved in 3 mL of acetonitrile in a 10-mL flask attached to a vacuum line and gas buret. Pure dioxygen was added to the mixture at the desired pressure in a series of three freeze–thaw cycles. The temperature of the flask was then brought to the required temperature by a constant-temperature bath, and the reaction was started by injection of 3 mmol of α-terpinene into the reaction mixture. Samples were taken at the appropriate intervals and immediately analyzed by GLC under the conditions given above. When necessary, the rate of dioxygen consumption was also measured volumetrically by use of the gas buret.

**Redox Reaction of the $H_5PV_2Mo_{10}O_{40}$ Catalyst.** The reduction and oxidation reaction of the $H_5PV_2Mo_{10}O_{40}$ catalyst by α-terpinene was followed by UV–vis spectroscopy. For catalyst reduction, a stirred 1.5 mM solution of $H_5PV_2Mo_{10}O_{40}$ in acetonitrile at constant temperature was reduced by addition of 2 equiv of α-terpinene and the absorption spectra was measured every 0.5 s. For catalyst reoxidation, a stirred 20 mM solution of $H_5PV_2Mo_{10}O_{40}$ in acetonitrile under pure dioxygen or air at constant temperature was reduced by the appropriate amount of α-terpinene. After maximum absorption had been achieved (about 30 s), the catalyst reoxidation was measured by the disappearance of the heteropoly blue peak at intervals of 15 s.

**Oxidative Dehydrodimerization of Dialkylphenols.** The reactions were performed by mixing 1 mmol of substrate and 0.02 mmol of $H_5PV_2Mo_{10}O_{40}$ in 20 mL of ethanol at 1 atm of dioxygen and at 60 °C for 4 h. Conversions were computed by HPLC analysis using a RP-18 reversed-phase column and using 10% dichloromethane in 1-hexanol as eluent at a flow rate of 1 mL/min.

**Electron Spin Resonance Spectra.** Solutions for ESR spectra were prepared by mixing the appropriate amounts of catalyst and reducing agent (α-terpinene or iron(II) sulfate) in acetonitrile. The specific conditions for each spectrum are given in the figure captions.

**Phosphorus-31 NMR Spectra.** Solutions of 20 mM heteropolyanions were prepared in 1/4 $CD_3CN/CH_3CN$ and their spectra recorded (500 pulses) at room temperature. Peaks are relative to $H_3PO_4$ as the external standard.

**Infrared Spectra.** Infrared spectra were taken only of dried samples. Thus, the hydrated catalyst was dried under vacuum at 150 °C for 24 h. The $^{18}O$-substituted catalyst was prepared by adding a 100 molar excess of $H_2{}^{18}O$ to a dried catalyst until the catalyst redissolved. The excess water was evaporated; the procedure was repeated two more times and the catalyst dried as above. Samples for IR analysis were prepared by dissolving the catalyst in a small amount (with or without addition of α-terpinene) of dried acetonitrile and quickly revaporating the solvent on the NaCl plate.

**Acknowledgment.** We thank the Wolfson Foundation for Scientific Research for funding this project, Professor J. Blum for his assistance and suggestions, and Professor H. Levanon for the use of the ESR spectrometer.

(44) Sheldon, R. A.; Kochi, J. K. *Metal Catalyzed Oxidations of Organic Compounds*; Academic Press: New York, 1981.
(45) Yurchenko, E. N.; Miessner, H.; Trunschke, A. *J. Struct. Chem. (Engl. Transl.)* **1989**, *30*, 22.
(46) (a) Klemperer, W.; Shum, G. *J. Am. Chem. Soc.* **1978**, *100*, 4891. (b) Maksimovskaya, R. I.; Subocheva, O. A.; Kuznetsova, L. I. *Izv. Akad. Nauk SSSR Ser. Khim.* **1986**, *10*, 2167.
(47) Tsigdinos, G. A.; Hallada, C. J. *Inorg. Chem.* **1968**, *7*, 437.